Title	Room temperature electromechanical and magnetic investigations of ferroelectric Aurivillius phase Bi5Ti3(FexMn1−x)O15 (x= and 0.7) chemical solution deposited thin films
Authors	Keeney, Lynette;Groh, Claudia;Kulkarni, Santosh;Roy, Saibal;Pemble, Martyn E.;Whatmore, Roger W.
Publication date	2012-07
Original Citation	Keeney, L., Groh, C., Kulkarni, S., Roy, S., Pemble, M. E. and Whatmore, R. W. (2012) 'Room temperature electromechanical and magnetic investigations of ferroelectric Aurivillius phase Bi5Ti3(FexMn1−x)O15 (x= and 0.7) chemical solution deposited thin films', Journal of Applied Physics 112(2), 024101. http://dx.doi.org/10.1063/1.4734983
Type of publication	Article (peer-reviewed)
Link to publisher's version	10.1063/1.4734983
Rights	© 2012 American Institute of Physics. This article may be downloaded for personal use only. Any other use requires prior permission of the author and AIP Publishing. The following article appeared in L. Keeney et al. J. Appl. Phys. 112, 024101 (2012) and may be found at http://dx.doi.org/10.1063/1.4734983
Download date	2025-07-27 17:34:44
Item downloaded from	https://hdl.handle.net/10468/2990

Room temperature electromechanical and magnetic investigations of ferroelectric Aurivillius phase Bi5Ti3(FexMn1−x)O15 (x=1 and 0.7) chemical solution deposited thin films

Lynette Keeney, Claudia Groh, Santosh Kulkarni, Saibal Roy, Martyn E. Pemble et al.

Related Articles

Evidence of temperature dependent domain wall dynamics in hard lead zirconate titanate piezoceramics
J. Appl. Phys. 112, 014113 (2012)

Fabrication and properties of radially 001C textured PMN-PT cylinders for transducer applications
J. Appl. Phys. 112, 014105 (2012)

Shift of morphotropic phase boundary in high-performance [111]-oriented epitaxial Pb (Zr, Ti) O3 thin films
J. Appl. Phys. 112, 014102 (2012)

Frequency-dependence of large-signal properties in lead-free piezoceramics
J. Appl. Phys. 112, 014101 (2012)

Mechanical characterization of an electrostrictive polymer for actuation and energy harvesting
J. Appl. Phys. 111, 124115 (2012)
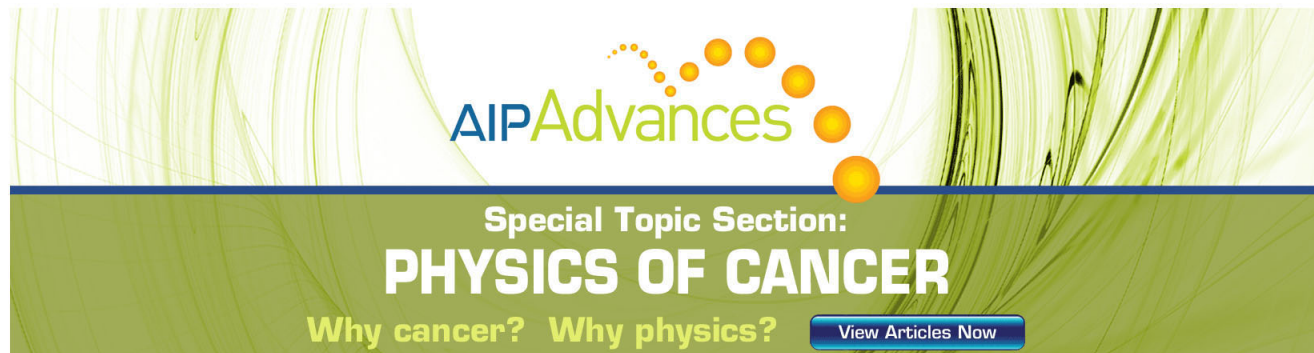
Additional information on J. Appl. Phys.

Journal Homepage: http://jap.aip.org/

Journal Information: http://jap.aip.org/about/about_the_journal

Top downloads: http://jap.aip.org/features/most_downloaded

Information for Authors: http://jap.aip.org/authors

Room temperature electromechanical and magnetic investigations of ferroelectric Aurivillius phase $Bi_5Ti_3(Fe_xMn_{1-x})O_{15}$ (x = 1 and 0.7) chemical solution deposited thin films

Lynette Keeney,[1,a)] Claudia Groh,[2] Santosh Kulkarni,[1] Saibal Roy,[1] Martyn E. Pemble,[1] and Roger W. Whatmore[1]

[1]*Tyndall National Institute, University College Cork, 'Lee Maltings', Dyke Parade, Cork, Ireland*
[2]*Materials Science Department, Friedrich Schiller University of Jena, Jena, Germany*

Aurivillius phase thin films of $Bi_5Ti_3(Fe_xMn_{1-x})O_{15}$ with $x = 1$ ($Bi_5Ti_3FeO_{15}$) and 0.7 ($Bi_5Ti_3Fe_{0.7}Mn_{0.3}O_{15}$) on SiO_2-Si(100) and Pt/Ti/SiO_2-Si substrates were fabricated by chemical solution deposition. The method was optimized in order to suppress formation of pyrochlore phase $Bi_2Ti_2O_7$ and improve crystallinity. The structural properties of the films were examined by x-ray diffraction, scanning electron microscopy, and atomic force microscopy. Optimum crystallinity and pyrochlore phase suppression was achieved by the addition of 15 to 25 mol. % excess bismuth to the sols. Based on this study, 17.5 mol. % excess bismuth was used in the preparation of $Bi_2Ti_2O_7$-free films of $Bi_5Ti_3FeO_{15}$ on $SrTiO_3$(100) and $NdGaO_3$(001) substrates, confirming the suppression of pyrochlore phase using this excess of bismuth. Thirty percent of the Fe^{3+} ions in $Bi_5Ti_3FeO_{15}$ was substituted with Mn^{3+} ions to form $Bi_2Ti_2O_7$-free thin films of $Bi_5Ti_3Fe_{0.7}Mn_{0.3}O_{15}$ on Pt/Ti/SiO_2-Si, SiO_2-Si(100), $SrTiO_3$(100), and $NdGaO_3$(001) substrates. $Bi_5Ti_3FeO_{15}$ and $Bi_5Ti_3Fe_{0.7}Mn_{0.3}O_{15}$ thin films on Pt/Ti/SiO_2-Si and SiO_2-Si(100) substrates were achieved with a higher degree of *a*-axis orientation compared with the films on $SrTiO_3$(100) and $NdGaO_3$(001) substrates. Room temperature electromechanical and magnetic properties of the thin films were investigated in order to assess the potential of these materials for piezoelectric, ferroelectric, and multiferroic applications. Vertical piezoresponse force microscopy measurements of the films demonstrate that $Bi_5Ti_3FeO_{15}$ and $Bi_5Ti_3Fe_{0.7}Mn_{0.3}O_{15}$ thin films are piezoelectric at room temperature. Room temperature switching spectroscopy-piezoresponse force microscopy measurements in the presence and absence of an applied bias demonstrate local ferroelectric switching behaviour (180°) in the films. Superconducting quantum interference device magnetometry measurements do not show any room temperature ferromagnetic hysteresis down to an upper detection limit of 2.53×10^{-3} emu; and it is concluded, therefore, that such films are not mutiferroic at room temperature. Piezoresponse force microscopy lithography images of $Bi_5Ti_3Fe_{0.7}Mn_{0.3}O_{15}$ thin films are presented. © *2012 American Institute of Physics*. [http://dx.doi.org/10.1063/1.4734983]

I. INTRODUCTION

Due to toxicological and environmental concerns, there is an increasing need for lead-free materials for use as piezoelectric actuators, sensors, and transducers, especially for use at elevated temperatures in applications, such as internal combustion engines.[1] Bismuth layer-structured ferroelectric materials in the Aurivillius phase[2] have received increasing interest as lead free piezoelectric materials with high ferroelectric Curie temperatures (T_c generally over 500 °C).[3,4] Because of their fatigue-free nature, Aurivillius phase materials have also been given significant attention for their potential use in ferroelectric random-access memory (FeRAM),[5,6] which combines the speed of dynamic access memory (DRAM) with the non-volatility and lower power requirements of hard disk and flash memory.[5–9] These materials are naturally 2D nanostructured in nature, consisting of $(Bi_2O_2)^{2+}$ layers alternating with $nABO_3$ per-

ovskite units, in blocks ∼1–2 nm thick, described by the general formula $Bi_2O_2(A_{n-1}B_nO_{3n+1})$.

The layered nature of these materials also allows for the incorporation of magnetic ions with +3 to +5 oxidation states[10] in the *B* sites of the perovskite units, potentially allowing cations that drive both ferroelectricity (unoccupied *d* orbitals) and ferromagnetism (partially filled *d* orbitals) to occupy adjacent perovskite units. In this way, the normally conflicting electronic structure requirements[11] for single phase multiferroics could potentially be accommodated. $BiFeO_3$ has been shown to exhibit coupled ferroelectric and antiferromagnetic ordering at ambient temperatures.[12] However because this compound is antiferromagnetic, it cannot be switched by a magnetic field. The synthesis of novel room temperature single phase magnetoelectric multiferroic materials is particularly appealing, not only because they have properties of both parent compounds but also because magnetoelectric coupling interactions, either directly between the electric and magnetic order parameters or indirectly via strain, can lead to additional functionalities and could potentially lead to a new generation of magnetoelectric

memory devices that can be electrically written and magnetically read.[13,14] This potential to electrically control magnetism means that single-phase magnetoelectric multiferroic materials are of considerable interest for potential applications in spin based memory/logic devices.[15]

BiFeO$_3$ (anti-ferromagnetic when in the pure perovskite form)[16] can be inserted into the normally three-layered Aurivillius phase Bi$_4$Ti$_3$O$_{12}$. This increases the number of perovskite layers, m, to form compounds such as the four-layered structure, Bi$_5$Ti$_3$FeO$_{15}$ (BTFO).[17] On increasing the number of perovskite layers (m), the microstructural, ferroelectric, magnetic, and other physical properties of the Aurivillius phase materials can be altered significantly.[18] In fact, the coexistence of ferroelectric and weak ferromagnetic properties at room temperature has been reported for the four-layered Bi$_5$Ti$_3$FeO$_{15}$ materials in thin film form.[19,20] Mao *et al.*[21] reported enhanced multiferroic properties for the Bi$_5$Ti$_3$Fe$_{0.5}$Co$_{0.5}$O$_{15}$ ceramics by substituting *B* site Fe cations with Co cations, although a discussion of possible trace impurities that may contribute to the ferromagnetic results was absent in these articles.

Since enhanced electrical properties, positive magneto-capacitance effects, and suppressed leakage currents have been reported[22,23] for pervoskite-type structures substituted at the *B* site with Mn^{3+} cations, we previously devised a synthetic method for the preparation of BTFO and Mn^{3+} substituted Bi$_5$Ti$_3$Fe$_{0.7}$Mn$_{0.3}$O$_{15}$ (BTF7M3O) thin films.[24] Piezoresponse force microscopy (PFM) has been highly effective in the identification of these thin films as novel piezoelectric materials.[24] However, given the coexistence of pyrochlore phase Bi$_2$Ti$_2$O$_7$ in some of the films analyzed, it is expected that single-phase films would have enhanced piezoelectric properties. As yet, the magnetic properties of BTF7M3O thin films have not been reported.

In this study, we report an optimised chemical solution deposition method for the preparation of Bi$_2$Ti$_2$O$_7$ pyrochlore-free BTFO and BTF7M3O thin films and investigate the effect of substrate (Pt/Ti/SiO$_2$-Si, SiO$_2$-Si(100), SrTiO$_3$(100), and NdGaO$_3$(001)) on thin film crystallinity, phase purity, and morphology. The potential room temperature ferroelectric and multiferroic properties of Bi$_2$Ti$_2$O$_7$ pyrochlore-free BTFO and BTF7M3O thin films on Pt/Ti/SiO$_2$-Si, SiO$_2$-Si(100), SrTiO$_3$(100) (STO), and NdGaO$_3$(001) (NGO) substrates have been investigated by vertical PFM, switching spectroscopy PFM (SS-PFM), ferroelectric lithography, and SQUID (superconducting quantum interference device) magnetometry.

II. EXPERIMENTAL

Sols of BTFO and BTF7M3O were prepared by dissolving the required amounts of Bi(NO$_3$)$_3$·5H$_2$O (bismuth nitrate pentahydrate) and Ti(OCH$_2$CH$_2$CH$_2$CH$_3$)$_4$ (titanium(IV) butoxide) in lactic acid (CH$_3$CHOHCOOH) at room temperature. Fe(NO$_3$)$_3$·9H$_2$O (iron(III) nitrate nonahydrate) and Mn(C$_5$H$_7$O$_2$)$_3$ (manganese(III) acetylacetonate) as required were dissolved separately in acetylacteone (see Fig. 1). When complete dissolution was achieved, this solution was slowly dropped into the Bi^{3+}/Ti^{4+} solution under constant

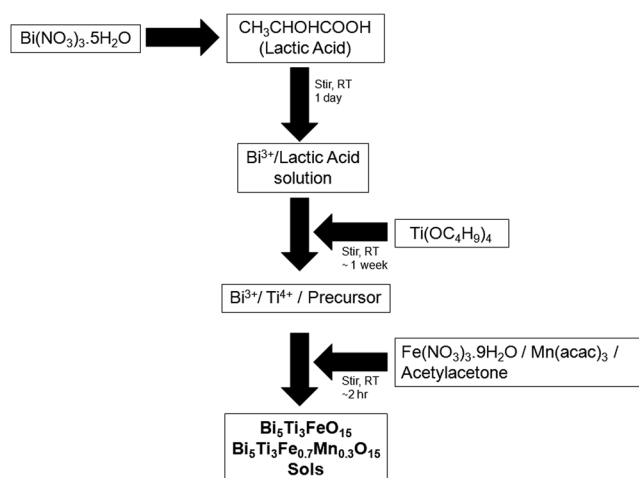

FIG. 1. Flow chart for the preparation of BTFO and BTF7M3O sols.

stirring to prepare 0.7 mol dm^{-3} sols of BTFO and BTF7M3O. The amount of excess bismuth added to the sols during preparation ranged from 0 to 35%.

BTFO and BTF7M3O thin films were spin coated on Pt/Ti/SiO$_2$/Si, SiO$_2$-Si (Si(100) with native oxide), STO, and NGO substrates by a commercial spinner operating at 4500 rpm for 30 s (spin coater KW-4A, Chemat Technology) yielding films of thicknesses of ~100 nm for each spin-coated layer deposited, as observed in cross-section SEM measurements. Excess solvents and residual organics were removed from the films by baking on a calibrated hot plate at 300 ± 5.0 °C for approximately 10 min. The films were crystallised by annealing in ambient air at 800 °C (BTF7M3O) or 850 °C (BTFO) for 1 h in a conventional furnace.

X-ray diffraction (XRD) profiles were recorded at room temperature using a Phillips Xpert PW3719 MPD diffractometer, equipped with a Cu-Kα radiation source (40 kV and 35 mA) and a nickel filter on the incident beam over the range $5° \leq 2\theta \leq 37.5°$.

Topography was examined using high resolution scanning electron microscopy (HRSEM) and atomic force microscopy (AFM). SEM images and energy dispersive x-ray (EDX) analysis spectra were obtained using a FEI Nova 630 High Resolution Scanning Electron Microscope. A commercial atomic force microscope (MFP-3D, Asylum Research) in ac (alternating current) mode (intermittent contact mode) was used for topography mapping of the films. Olympus AC240TS/AC160TS silicon cantilevers (Al reflex coated, ~70/300 kHz resonant frequency, respectively) were used for imaging.

Electromechanical responses of the films were measured by PFM using the AFM in contact mode equipped with a HVA220 Amplifier for PFM. Out-of-plane electromechanical responses of the films were investigated by the Dual AC Resonance Tracking Piezoresponse Force Microscopy (DART-PFM)[25] mode. Vertical DART-PFM hysteresis loop measurements were obtained by SS-PFM (Refs. 26–28) using a triangle step waveform (comprised pulse dc (direct current) bias voltage (16.5 V) and an ac signal (5.5 V)). The waveform was cycled twice at a frequency of 0.4 Hz with 48

ac steps per waveform. Olympus AC240TM electrilevers, Ti/Pt coated silicon cantilevers (Al reflex coated, 70 kHz resonant frequency, ~320 kHz contact resonance frequency) were used for PFM imaging and the inverse optical lever sensitivity (InVOLS) of the cantilevers was calibrated according to the MFP-3D Procedural Operation "Manualette." Ferroelectric lithography was performed using the PFM lithography mode by converting an imported grey-scale image into a bias map.

Room temperature magnetic measurements of the thin films were carried out using a Quantum Design SQUID magnetometer (Quantum Design USA; Model—MPMS XL5) over an applied magnetic field range of ±5000 Oe. The film weight was estimated from sample area and film thickness measurements (determined from HRSEM measurements), combined with the x-ray density to be 1.29×10^{-5} g.

III. RESULTS AND DISCUSSION

A. Studies on effect of excess bismuth on BTFO thin film crystallinity

Previous work reported[24] the crystallization of BTFO thin films on Pt/Ti/SiO$_2$-Si substrates at annealing temperatures of 850 °C. With 5% excess bismuth, however, the presence of impurity pyrochlore phase $Bi_2Ti_2O_7$ is evident, as indicated by the presence of the (222) and (444) reflections.[24] Studies on the addition of between 0 and 35% excess bismuth to the BTFO sols demonstrate that the addition of at least 5% excess bismuth improves BTFO phase crystallinity and decreases the formation of $Bi_2Ti_2O_7$ pyrochlore phase (Joint Committee for Powder Diffraction Standard (JCPDS) No. 32-0118) in BTFO films on Si(100) (Fig. 2(a)) and Pt/Ti/SiO$_2$-Si (Fig. 2(b)) substrates. Optimum crystallinity and pyrochlore phase suppression is achieved by the addition of between 15 and 25 mol. % excess bismuth. Addition of further bismuth excess leads to the formation of secondary phase peaks, including peaks which match to the reflections of the impurity phases Bi_2SiO_5 (JCPDS No. 75-1483) and Bi_4SiO_3 (JCPDS No. 88-0243). It is likely that at the processing conditions used for crystallizing the main phase (850 °C) and having an excess of Bi in the film, a reaction between Bi_2O_3 and SiO_2 occurs at the interface between the film and substrate to form the observed bismuth-silicate phases[29–32] on cooling.

SEM images reveal grain structures crystallised in plate-like morphologies, which is characteristic of the layered Aurivillius-type structures (Fig. 3). Due to the layered nature of the grains, cross-sectional SEM images (Fig. 3(b)) reveal varying thicknesses across the course of the films, with average thickness of ~100 nm. AFM images are complementary to the XRD data, where grain size increases and the characteristic Aurivillius-type layer structures are revealed for 0 to 15% excess bismuth addition (Fig. 4). With further bismuth excess, however, both smaller and larger secondary phase structures are evident, in addition to the Aurivillius phase plate-like structures.

Based on this study of the optimisation of BTFO on Pt/Ti/SiO$_2$-Si and Si(100) substrates, 17.5 mol. % excess bismuth (>15% but <25% excess bismuth) was used to prepare
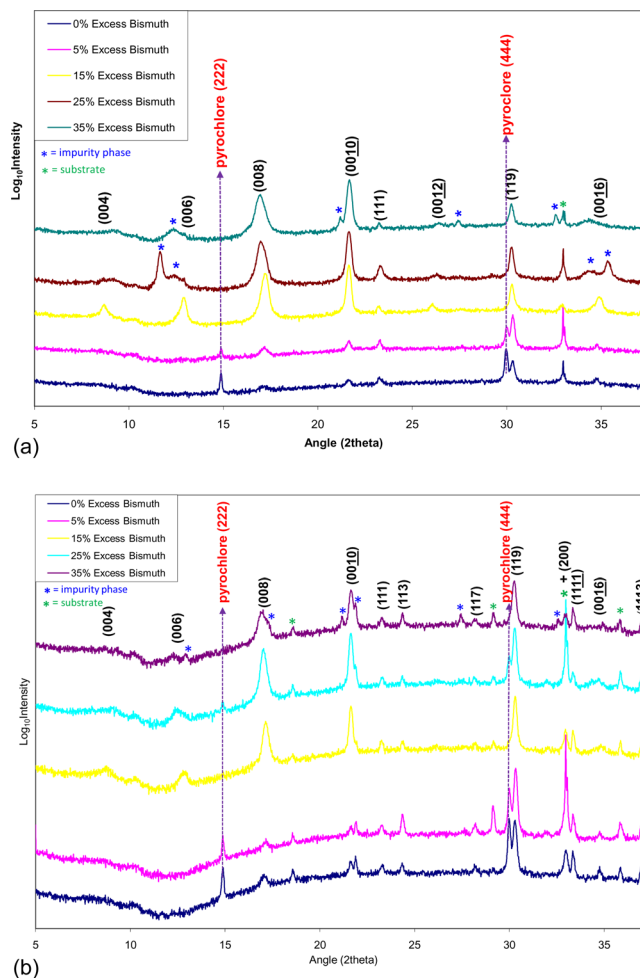

FIG. 2. Effect of addition of 0 to 35% excess bismuth during preparation on the XRD patterns of BTFO thin films on (a) Si(100) and (b) Pt/Ti/SiO$_2$-Si substrates annealed at 850 °C.

thin films of BTFO on SrTiO$_3$(100) and NdGaO$_3$(001) substrates and BTF7M3O thin films on Pt/Ti/SiO$_2$-Si, SiO$_2$-Si(100), SrTiO$_3$(100), and NdGaO$_3$(001) substrates.

B. Studies on effect of substrate on BTFO and BTF7M3O thin film crystallinity

Investigations on the growth of BTFO (Fig. 5) and BTF7M3O (Fig. 6) thin films on Pt/Ti/SiO$_2$-Si, SiO$_2$-Si(100), NdGaO$_3$(001), and SrTiO$_3$(100) substrates demonstrate that films of the $m = 4$ Aurivillius phase (JCPDS No. 38-1257), free from $Bi_2Ti_2O_7$ pyrochlore phase, were obtained at annealing temperatures of 850 and 800 °C, respectively. This demonstrates that 17.5 mol. % excess bismuth is sufficient for suppressing pyrochlore phases in the films on the substrates studied. EDX analysis spectra confirmed that manganese was successfully inserted into the Aurivillius structures of BTF7M3O. The relative intensities of the (00l) reflections are greater on SrTiO$_3$(100) and NdGaO$_3$(001) substrates than on the Pt/Ti/SiO$_2$/Si and SiO$_2$-Si(100) substrates. In general, the full-width at half maximum (FWHM) values of the (00l) reflections decrease in the order SiO$_2$/Si or Pt/Ti/SiO$_2$-Si > NdGaO$_3$(001) > SrTiO$_3$(100). The relative intensities of the (200) reflections for the BTFO and BTF7M3O thin films
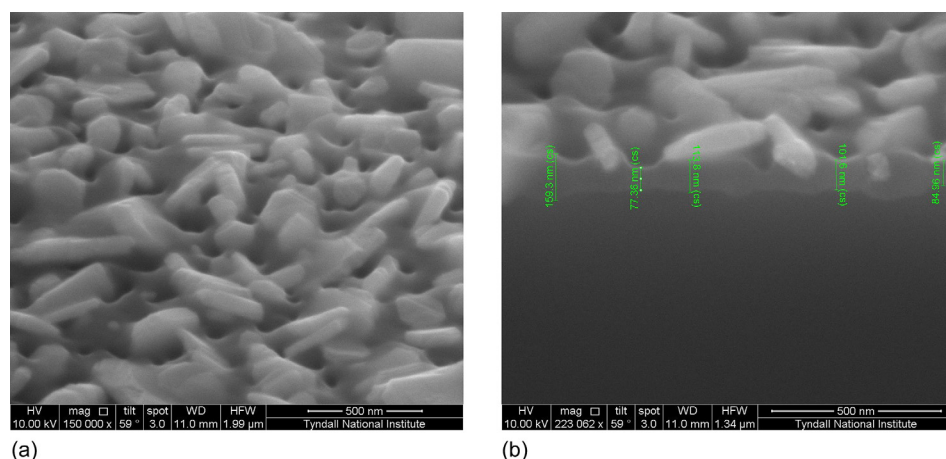
(a)

(b)

FIG. 3. Representative (a) top-view and (b) cross-section HRSEM images of BTFO thin film on SiO$_2$-Si(100) annealed at 850 °C. 17.5% excess Bi was used during preparation.

are highest on the SiO$_2$-Si(100) substrates. The intensity ratio between a (h00) and a (00l) peak is a measure of the content of the phase with *a*-axis orientation. Using the data in Fig. 5, ratios of the (200) and the (00$\underline{16}$) peaks (I$_{200}$/I$_{00\underline{16}}$) are determined to be 0.0181, 0.0310, 1.589, and 1.296 for BTFO on STO, NGO, SiO$_2$/Si, and Pt/Ti/SiO$_2$-Si, respectively. The data in Fig. 6 present values of 0.0452, 0.0599, 21.35, and 16.140 for the ratios of the (200) vs. (00$\underline{16}$) peaks (I$_{200}$/I$_{00\underline{16}}$) for BTF7M3O on STO, NGO, SiO$_2$/Si, and Pt/Ti/SiO$_2$-Si, respectively. The x-ray diffraction data thus indicate that the crystals in BTFO and BTF7M3O films grown on SrTiO$_3$(100) exhibit a significantly greater degree of *c*-axis orientation.

The impurity peaks noted for the BTFO films on SrTiO$_3$(100) and NdGaO$_3$(001) are possibly due to the presence of the non-ferroelectric pyrochlore phase Bi$_2$Fe$_4$O$_9$ (orthorhombic; JCPDS No. 74-1098). A possible match for the peak at the 2θ value of 14.3° is the (008) reflection of

Bi$_6$Ti$_3$FeO$_{18}$. The unidentified peaks in the BTF7M3O films do not correspond to the peaks observed by Ahn *et al.*,[33] corresponding to the structural change from Bi$_5$Ti$_3$FeO$_{15}$ in the case of Bi$_5$Ti$_3$Fe$_{1-x}$Mn$_x$O$_{15}$ ceramics where x $\geq$ 0.5. Obvious oxide phases do not account for the unidentified peaks in the BTFO and BTF7M3O thin films.

Layered grains of different orientations overlapping one another can also be seen in the AFM images of the BTF7M3O films (Fig. 7). AFM images are complimentary to the x-ray diffraction data (Fig. 6), where it can be seen that BTF7M3O grain size increases in the order SiO$_2$-Si < Pt < NGO < STO films.

C. Ferroelectric investigations using vertical DART-PFM switching spectroscopy-PFM

Previous single frequency PFM investigations[35] demonstrate that the films are piezoelectric at room temperature
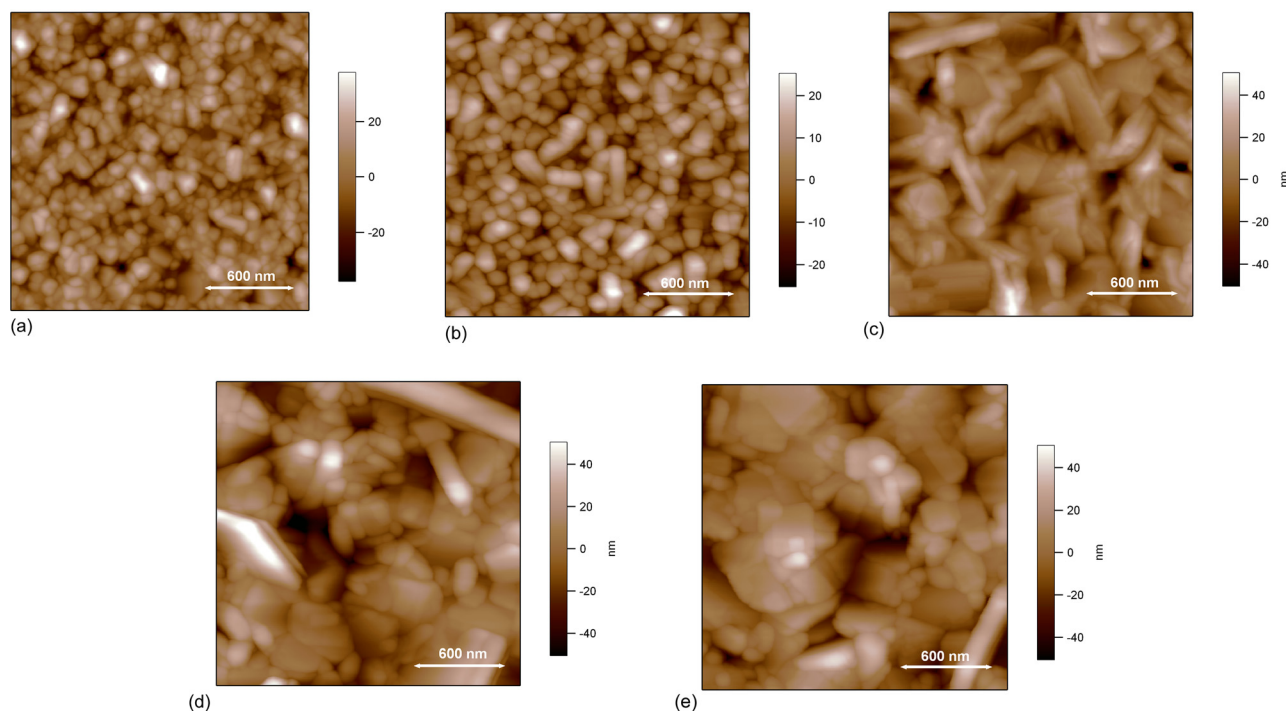

(a)

(b)

(c)

(d)

(e)

FIG. 4. Representative AFM images of BTFO thin films on SiO$_2$-Si(100) annealed at 850 °C with (a) 0%, (b) 5%, (c) 15%, (d) 25%, (e) 35% excess Bi addition during preparation.
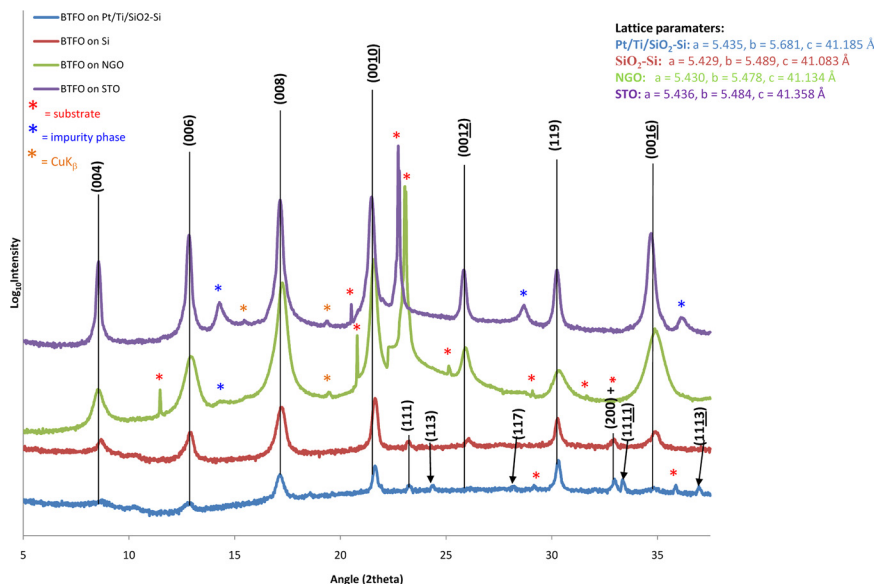
FIG. 5. XRD patterns of BTFO on Pt/Ti/SiO$_2$-Si, SiO$_2$-Si(100), NdGaO$_3$(001), and SrTiO$_3$(100) substrates annealed at 850 °C.

with the major polarization vector in the lateral plane of the films, as is characteristic[34] for Aurivillius phase materials. Vertical PFM measurements were carried out using the DART-PFM mode. This technique uses the cantilever resonance frequency to boost the piezo signal in the vertical direction, while reducing crosstalk between changes in the sample-tip contact stiffness and the PFM signal by tracking the resonance frequency based on amplitude detection feedback.[25] The amplitude is measured at one drive frequency below the resonance frequency and another above it. The error signal allows changes in the resonance frequency to be tracked, thereby reducing the effects of cross-talk between PFM signal and changes in the sample-tip contact stiffness. Representative images of the vertical electromechanical nature of the films investigated by the DART-PFM technique are shown in Fig. 8. Since DART mode uses the contact resonance to amplify the piezo-response signal, the piezo-response measured will be larger than the unamplified piezo-response. However, since the gain on this amplification is

likely to change over the surface, extraction of absolute values piezo-response from these images was not conducted. Vertical PFM response appears to arise from *a*-axis oriented grains (Figs. 5 and 6). These grains have their crystallographic *a*-axis tilted out-of-plane and are therefore accessible to probing by vertical PFM. No significant vertical PFM response was observed for BTFO thin films on SrTiO$_3$, which are preferentially *c*-axis oriented.

PFM switching spectroscopy can locally generate hysteresis loops and thereby provide information on local ferroelectric switching behaviour. During acquisition of a hysteresis loop, the conducting PFM tip is fixed at a given location on the sample surface and a triangle-step bias waveform (comprised pulse dc bias voltage and an ac signal) is applied.[26–28] Vertical DART-PFM switching spectroscopy hysteresis loops were generated at room temperature in the presence and absence of an applied dc bias at different points across the BTFO and BTF7M3O thin films. Flat, *c*-axis oriented grains did not display hysteresis, while tilted (*a/b*-axis oriented)
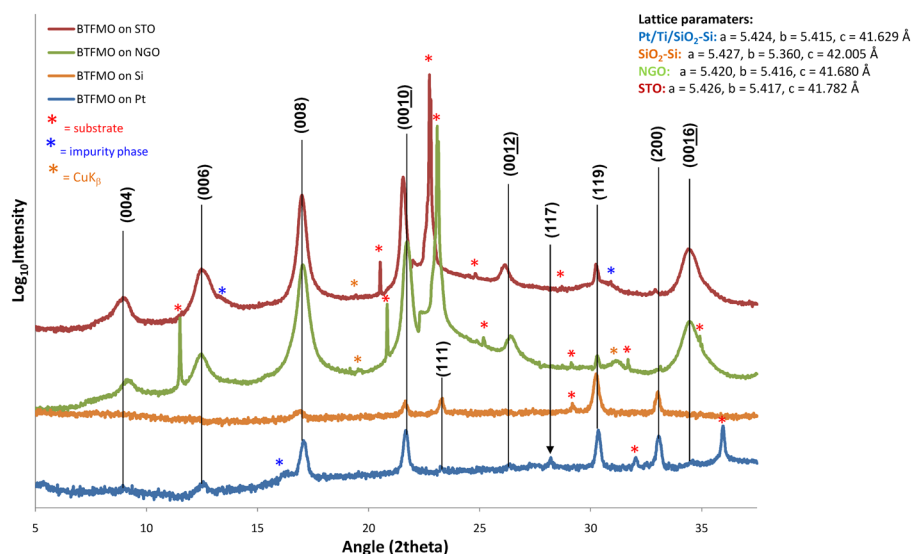

FIG. 6. XRD patterns of BTF7M3O on Pt/Ti/SiO$_2$-Si, SiO$_2$-Si(100), NdGaO$_3$(001), and SrTiO$_3$(100) substrates annealed at 800 °C.
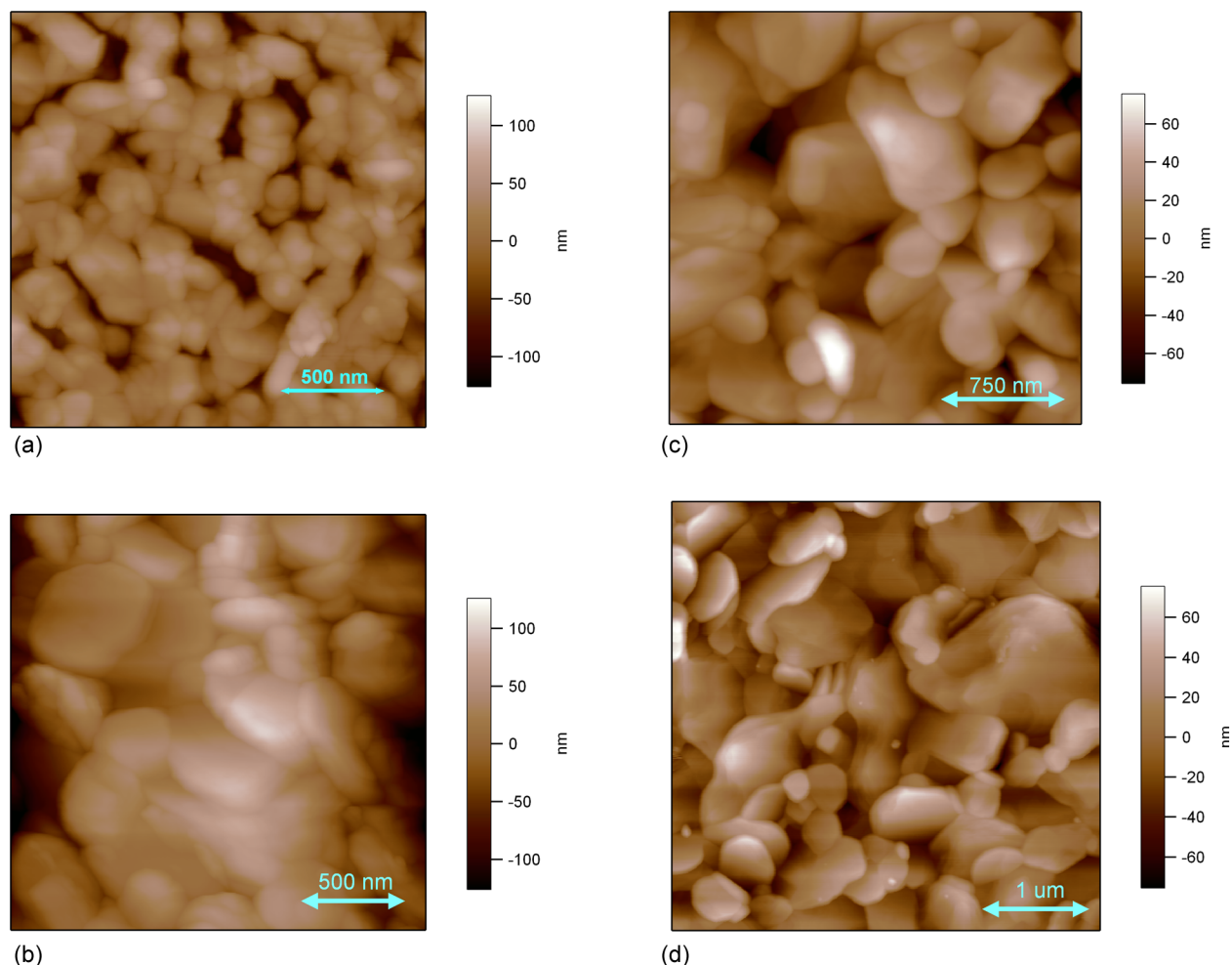
FIG. 7. Representative AFM images of BTF7M3O (annealed at 800 °C) on (a) SiO$_2$-Si(100), (b) Pt/Ti/SiO$_2$-Si, (c) NdGaO$_3$, and (d) SrTiO$_3$ substrates.

grains demonstrated 180° ferroelectric switching behaviour. Local ferroelectric switching was demonstrated for both sets of films, with the exception of BTFO thin films on SrTiO$_3$. Local remanent DART-PFM hysteresis loops for BTFO and BTF7M3O thin films on Pt/Ti/SiO$_2$-Si substrates, clearly demonstrating ferroelectric switching, are shown in Fig. 9.

D. Ferroelectric lithography investigations

When an applied dc field from the PFM probe is greater than the ferroelectric coercive field of a thin film sample, it can induce ferroelectric polarization reversal. The PFM lithography mode uses this technique to vertically "write" single domains, domain arrays, and complex patterns without changing the surface topography. The "read" operation involves PFM detection of written domains. X-ray diffraction patterns demonstrated that the degree of *a*-axis orientation of the BTF7M3O thin films on SiO$_2$-Si was higher than that of the other films investigated; therefore, this sample was the most suitable candidate to probe vertical polarization reversal along the *a*-axis, where the major polarization vector of the Aurivillius phase materials lies. Furthermore, this
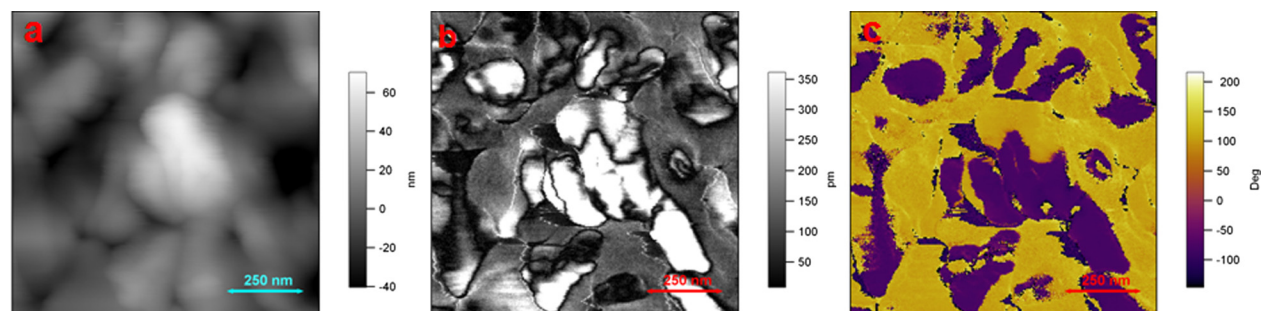

FIG. 8. (a) Topography image of BTFO thin film on Si substrate. (b) DART-PFM amplitude and (c) DART-PFM phase images of BTFO thin film on Si substrate.
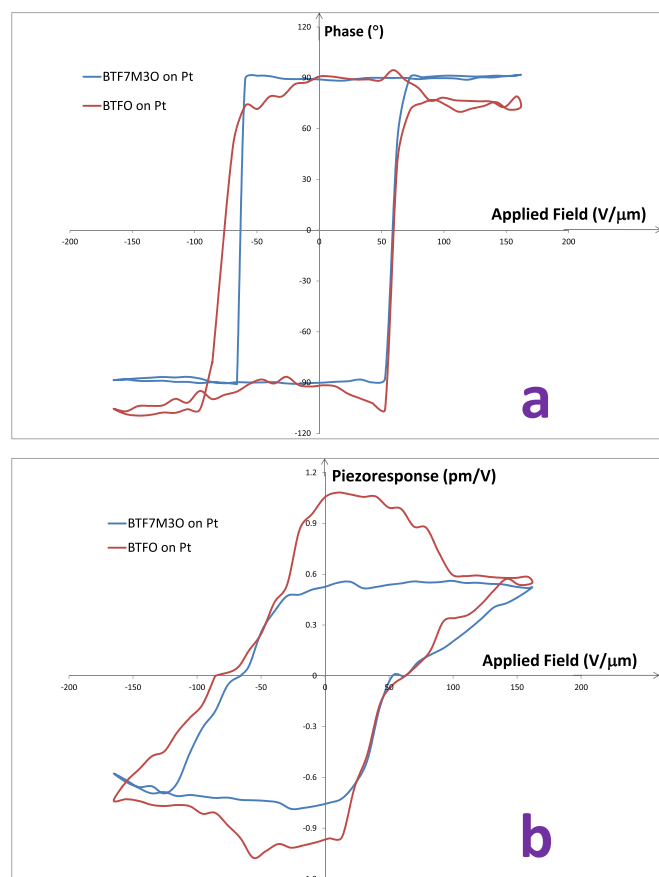
FIG. 9. Vertical DART-PFM switching spectroscopy (a) phase and (b) piezoresponse loops of BTFO and BTF7M3O thin films on Pt/Ti/SiO₂-Si in the absence of an applied DC bias.

film is single-phase Aurivillius. No impurity phase peaks are noted in this film, which could otherwise decrease the electromechanical response of piezoelectric films. By applying a dc bias of 16.5 V (applied field 165 V/μm) vertically to an area of the BTF7M3O thin films ("write" step), ferroelectric polarization reversal over areas of the film was achieved as detected by the subsequent PFM scan ("read" step), as is demonstrated in Figures 10 and 11. Tests conducted over an 8 h period demonstrated that the films retain polarization for this finite period of time.

E. Magnetic investigations using SQUID magnetometry

In-plane magnetic measurements of BTFO thin films on SrTiO₃ and BTF7M3O thin films on SrTiO₃ and Pt/Ti/SiO₂-Si substrates (Aurivillius phase film thickness ∼100 nm) were carried out at room temperature using a SQUID magnetometer over an applied magnetic field range of ±5000 Oe. No net magnetization was observed for the in-plane magnetization (M) vs. applied magnetic field (H) measurements of the BTFO and BTF7M3O thin films down to an upper detection limit of 2.53×10^{-3} emu (196 emu/g), which implies both a lack of ferromagnetic behaviour in the Aurivillius phase and the absence of any ferromagnetic phase impurities within the sample, which are difficult to detect at low levels (see supplementary material Fig. S1 (Ref. 38)). Given the absence of ferro/ferri-magnetic hysteresis, it is concluded that the BTFO and BTF7M3O thin films investigated do not show room temperature multiferroic behaviour. This is at-odds with some results published in the literature[19,20,36] which indicate some evidence for weak ferromagnetism in BTFO thin films and bulk ceramics at room temperature, although there is some variance in the reported saturation magnetization (M_s) values (e.g., M_s ranges from ∼0.21 to 3.1 emu/cm³ for the BTFO thin films). The occurrence of weak ferromagnetic behaviour in these compounds was attributed to local ferromagnetic Fe-O-Fe interactions; therefore, random distribution of the iron-oxygen and titanium-oxygen octahedra in the different BTFO compounds investigated may account for the variation in the observed magnetic behaviour. On the other hand, our previous investigations of the $Bi_5Ti_3Fe_{0.7}Co_{0.3}O_{15}$ thin films[35] and $Bi_5Ti_3Fe_{0.5}Co_{0.5}O_{15}$ ceramic samples[37] demonstrated that the observed ferromagnetic response was accounted for by the presence of trace amounts of second-phase ferromagnetic inclusions (undetected by x-ray diffraction measurements), whereas no magnetic response from the main Aurivillius phase was detectable. The previous reports[19,20,36] of ferromagnetic response in BTFO do not discuss the possibility of spinel phases such as iron oxide contributing to the ferromagnetic response observed. Given the absence of ferromagnetic hysteresis in the films studied here, the variance in the previously reported values and since trace amounts of magnetic impurities could lead to the magnetization values obtained, detailed analysis for possible magnetic impurity phases, and analysis of their effects should be performed before denoting
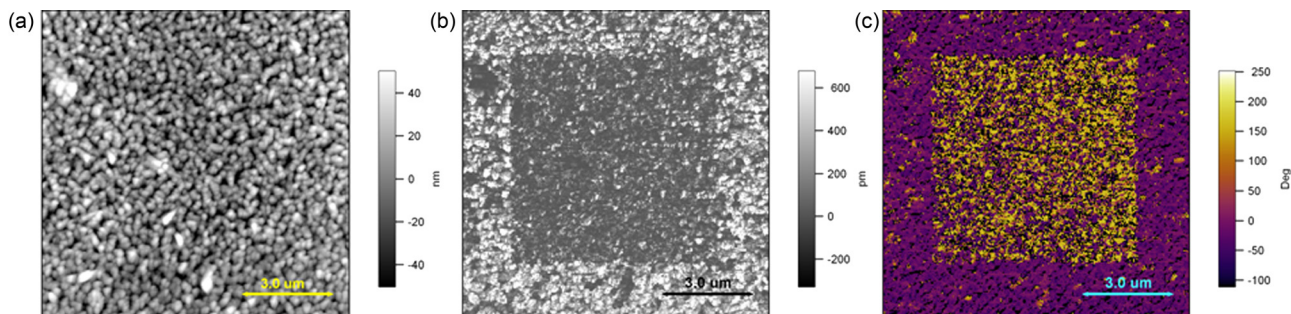

FIG. 10. Images of BTF7M3O on SiO₂-Si: (a) topography, (b) out-of-plane PFM amplitude, and (c) out-of-plane PFM phase after PFM lithography with an applied dc bias of 16.5 V.

FIG. 11. Images of BTF7M3O on SiO_2-Si: (a) topography, (b) out-of-plane PFM amplitude, and (c) out-of-plane PFM phase after PFM lithography with an applied dc bias of 33.0 V.

the $Bi_5Ti_3FeO_{15}/Bi_5Ti_3Fe_{0.7}Mn_{0.3}O_{15}$ materials as being ferromagnetic.

IV. CONCLUSIONS

Thin films of Aurivillius phase BTFO and BTF7M3O ($m = 4$), free from the non-ferroelectric $Bi_2Ti_2O_7$ pyrochlore phase, were synthesized on Pt/Ti/SiO_2-Si, SiO_2-Si(100), $NdGaO_3$(001), and $SrTiO_3$(100) substrates by an optimized chemical solution deposition method (using 17.5% excess bismuth). Minor impurity phase peaks were observed for BTFO films on NGO and STO and BTF7M3O films on Pt, NGO, and STO. BTFO and BTF7M3O thin films on Pt/Ti/SiO_2-Si and SiO_2-Si(100) substrates were achieved with a higher degree of *a*-axis orientation compared with the films on $SrTiO_3$(100)/$NdGaO_3$(001) and thus most suited for probing piezoelectric/ferroelectric properties along the major polarization axis of the $m = 4$ Aurivillius phase.

Piezoresponse force microscopy measurements established that the BTFO and BTF7M3O thin films on Pt/Ti/SiO_2-Si, SiO_2-Si(100), $SrTiO_3$(100), and $NdGaO_3$(001) substrates are piezoelectric and ferroelectric at room temperature with the major polarization vector in the lateral plane of the films. However, the absence of a detectable ferromagnetic hysteresis loop in the SQUID magnetometry measurements indicates that the BTFO and BTF7M3O films are not room temperature multiferroics. Since room temperature ferroelectric switching was observed for the BTFO and BTF7M3O thin films, the $Bi_{m+1}Fe_{m-3}Ti_3O_{3m+3}$ Aurivillius phase system could act as a perfect precursor for multiferroic thin film materials via *B* site substitution using alternative magnetic cations. Indeed, the coexistence of ferroelectricity and ferromagnetism above room temperature has recently been reported[21] in the $Bi_5Ti_3Fe_{0.5}Co_{0.5}O_{15}$ ceramics.

Along with the potential commercial applications of these novel ferroelectric thin films as lead-free piezoelectrics for adverse environments, the ability of the ferroelectric BTFO and BTF7M3O thin films to exist in and switch between two polarized states and retain polarization for a finite period makes possible their application as the active component of energy efficient FeRAM capacitors. Ferroelectric lithography investigations of BTF7M3O on silicon demonstrate that polarisation information can be stored in the films and recovered by PFM.

[1]J. Rödel, W. Jo, K. T. P. Seifert, E.-M. Anton, T. Granzow, and D. Damjanovic, J. Am. Ceram. Soc. **92**(6), 1153–1177 (2009).
[2]B. Aurivillius, Ark. Kemi **1**, 499 (1949).
[3]A. Moure, A. Castro, and L. Pardo, Prog. Solid State Chem. **37**(1), 15–39 (2009).
[4]C.-M. Wang, J.-F. Wang, S. Zhang, and T. R. Shrout, J. Appl. Phys. **105**(9), 094110 (2009).
[5]C. A. P. de Araujo, J. D. Cuchiaro, L. D. McMillan, M. C. Scott, and J. F. Scott, Nature (London) **374**(6523), 627–629 (1995).
[6]B. H. Park, B. S. Kang, S. D. Bu, T. W. Noh, J. Lee, and W. Jo, Nature (London) **401**(6754), 682–684 (1999).
[7]S. Ducharme and A. Gruverman, Nature Mater. **8**(1), 9–10 (2009).
[8]R. Waser and A. Rudiger, Nature Mater. **3**(2), 81–82 (2004).
[9]P. Zubko and J.-M. Triscone, Nature (London) **460**(7251), 45–46 (2009).
[10]P. Boullay, G. Trolliard, D. Mercurio, J. M. Perez-Mato, and L. Elcoro, J. Solid State Chem. **164**(2), 252–260 (2002).
[11]N. A. Hill, J. Phys. Chem. B **104**(29), 6694–6709 (2000).
[12]J. Wang, J. B. Neaton, H. Zheng, V. Nagarajan, S. B. Ogale, B. Liu, D. Viehland, V. Vaithyanathan, D. G. Schlom, U. V. Waghmare, N. A. Spaldin, K. M. Rabe, M. Wuttig, and R. Ramesh, Science **299**(5613), 1719–1722 (2003).
[13]R. Ramesh, Nat. Nanotechnol. **5**(11), 761–762 (2010).
[14]J. F. Scott, Nature Mater. **6**(4), 256–257 (2007).
[15]V. R. Palkar, J. John, and R. Pinto, Appl. Phys. Lett. **80**(9), 1628–1630 (2002).
[16]P. Fischer *et al.*, J. Phys. C **13**(10), 1931 (1980).
[17]I. G. Ismailzade, V. I. Nesterenko, F. A. Mirishli, and P. G. Rustamov, Sov. Phys. Crystallogr. **12**, 400–404 (1967).
[18]S. Patri, R. Choudhary, and B. Samantaray, J. Electroceram. **20**(2), 119–126 (2008).
[19]W. Bai, Y. Q. Gao, J. Y. Zhu, X. J. Meng, T. Lin, J. Yang, Z. Q. Zhu, and J. H. Chu, J. Appl. Phys. **109**(6), 064901 (2011).
[20]S. Nakashima, Y. Nakamura, K. Y. Yun, and M. Okuyama, Jpn. J. Appl. Phys., Part 1 **46**(10B), 6952–6955 (2007).
[21]X. Mao, W. Wang, X. Chen, and Y. Lu, Appl. Phys. Lett. **95**(8), 082901 (2009).
[22]Y. Noguchi, K. Yamamoto, Y. Kitanaka, and M. Miyayama, J. Eur. Ceram. Soc. **27**(13–15), 4081–4084 (2007).
[23]C. H. Yang, T. Y. Koo, and Y. H. Jeong, Solid State Commun. **134**(4), 299–301 (2005).
[24]L. Keeney, P. F. Zhang, C. Groh, M. E. Pemble, and R. W. Whatmore, J. Appl. Phys. **108**(4), 042004 (2010).
[25]B. J. Rodriguez, C. Callahan, S. V. Kalinin, and R. Proksch, Nanotechnology **18**(47), 475504 (2007).
[26]S. Jesse, A. P. Baddorf, and S. V. Kalinin, Appl. Phys. Lett. **88**(6), 062908 (2006).
[27]S. Jesse, H. N. Lee, and S. V. Kalinin, Rev. Sci. Instrum. **77**, 073702 (2006).
[28]S. Jesse, B. J. Rodriguez, A. P. Baddorf, S. V. Kalinin, and M. Alexe, Microsc. Microanal. **13**(Supplement S02), 1582–1583 (2007).

[29]Q. Tian, X. Wang, C. Yu, H. Jiang, Z. Zhang, Y. Wang, and S. Lin, Sci. China, Ser. E: Technol. Sci. **52**(8), 2295–2301 (2009).

[30]F. Yiting, F. Shiji, S. Renying, and M. Ishii, Prog. Cryst. Growth Charact. Mater. **40**(1–4), 183–188 (2000).

[31]Z. G. Zhang, X. F. Wang, and Q. Q. Tian, Sci. Sintering **42**, 51–59 (2010).

[32]V. P. Zhereb and V. M. Skorikov, Inorg. Mater. **39**, Suppl. 2, S121–S145 (2003).

[33]S.-L. Ahn, Y. Noguchi, M. Miyayama, and T. Kudo, Mater. Res. Bull. **35**(6), 825–834 (2000).

[34]T. Watanabe and H. Funakubo, J. Appl. Phys. **100**(5), 051602 (2006).

[35]L. Keeney, S. Kulkarni, N. Deepak, M. Schmidt, N. Petkov, P. F. Zhang, S. Cavill, S. Roy, M. E. Pemble, and R. W. Whatmore, "Room Temperature Ferroelectric and Magnetic Investigations and Detailed Phase Analysis of Aurivillius Phase $Bi_5Ti_3Fe_{0.7}Co_{0.3}O_{15}$ Thin Films," J. Appl. Phys. (in press).

[36]X. Y. Mao, W. Wang, and X. B. Chen, Solid State Commun. **147**(5–6), 186–189 (2008).

[37]M. Palizdar, T. P. Comyn, M. B. Ward, A. P. Brown, J. Harington, S. Kulkarni, L. Keeney, S. Roy, M. E. Pemble, R. W. Whatmore, C. Quinne, S. H. Kilcoyne, and A. J. Bell, in *Applications of Ferroelectrics (ISAF/PFM), 2011 International Symposium on and 2011 International Symposium on Piezoresponse Force Microscopy and Nanoscale Phenomena in Polar Materials, Vancouver, BC, 24–27 July 2011* (IEEE, 2011), pp. 1–4.

[38]See supplementary material at http://dx.doi.org/10.1063/1.4734983 for in-plane room temperature in-plane M vs. H measurement of $Bi_5Ti_3Fe_{0.7}Mn_{0.3}O_{15}$ thin film on $Pt/Ti/SiO_2$-Si.